JACS
JOURNAL OF THE AMERICAN CHEMICAL SOCIETY
pubs.acs.org/JACS
Article

Covalent-Frameworked 2D Crown Ether with Chemical Multifunctionality

Jinseok Kim, Sungin Kim, Jinwook Park, Sungsu Kang, Dong Joo Seo, Namjun Park, Siyoung Lee, Jae Jun Kim, Won Bo Lee, Jungwon Park,* and Jong-Chan Lee*

Cite This: https://doi.org/10.1021/jacs.3c11182

ABSTRACT: Here, we present the synthesis and characterization of a novel 2D crystalline framework, named C_2O, which mainly consists of carbon and oxygen in a 2:1 molar ratio and features crown ether holes in its skeletal structure. The covalent-frameworked 2D crown ether can be synthesized on a gram-scale and exhibits fine chemical stability in various environments, including acid, base, and different organic solvents. The C_2O efficiently activates KI through the strong coordination of K^+ with crown ether holes in a rigid framework, which enhances the nucleophilicity of I^- and significantly improves its catalytic activity for CO_2 fixation with epoxides. The presence of C_2O with KI results in remarkable increases in CO_2 conversion from 5.7% to 99.9% and from 2.9% to 74.2% for epichlorohydrin and allyl glycidyl ether, respectively. Moreover, C_2O possesses both electrophilic and nucleophilic sites at the edge of its framework, allowing for the customization of physicochemical properties by a diverse range of chemical modifications. Specifically, incorporating allyl glycidyl ether (AGE) as an electrophile or ethoxyethylamine (EEA) as a nucleophile into C_2O enables the synthesis of **C_2O-AGE** or **C_2O-EEA**, respectively. These modified frameworks exhibit improved conversions of 97.2% and 99.9% for CO_2 fixation with allyl glycidyl ether, outperforming unmodified C_2O showing a conversion of 74.2%. This newly developed scalable, durable, and customizable covalent framework holds tremendous potential for the design and preparation of outstanding materials with versatile functionalities, rendering them highly attractive for a wide range of applications.

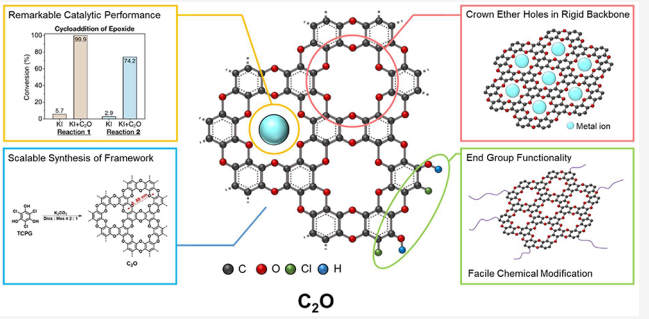

1. INTRODUCTION

The recent discovery of two-dimensional (2D) materials has garnered significant attention for various applications, such as separation,[1−3] gas storage,[4−7] electrodes,[8−12] and catalysis,[13−17] because of their high surface area, electrical/thermal conductivity, mechanical properties, and other beneficial properties. In particular, covalent organic frameworks (COFs), a class of 2D materials with a controlled porous structures, have been widely investigated in recent decades due to their tunable structures and properties.[18−20] The majority of current COFs have been synthesized by solvothermal methods that rely on dynamic chemistry (such as boronate ester,[21,22] hydrazone,[23] and imine linkage)[24,25] that involves reversible bond formation and breaking, allowing for the self-assembly of molecular building blocks into desired crystalline structures. However, these materials tend to have inherently low chemical stability due to their vulnerable covalent bonds. As a result, the synthesis of COFs is sensitive to small variations in reaction conditions, such as reactant ratios, reaction temperatures, and solvent selection. This limits their production scale to tens or a few hundred milligrams and hinders their utilization in practical applications.[26,27] To address these issues, the chemical stability has been improved by incorporating hydrogen bonds,[28] keto−enol tautomerism,[29] and interlayer interactions.[30] Gram-scale synthesis has been achieved by a solid-state coordination method and hydrothermal procedure.[31,32] Nevertheless, the development of chemically stable COFs exhibiting the desired functionality, especially in large-scale production, is still a major challenge for their practical applications.

COFs are solid materials based on organic frameworks. It implies that molecular chemical reactions, established in organic chemistry, can be employed to provide functionality while mechanical frameworks of the 2D materials are maintained. Crown ethers are macrocyclic host molecules that selectively bind alkali metal cations due to their electron-rich cavities.[33,34] The introduction of supramolecular "host−guest" chemistry of crown ethers has led to various applications in cation recognition,[35,36] biological systems,[37] and cataly-

Received: October 12, 2023
Revised: January 14, 2024
Accepted: January 20, 2024

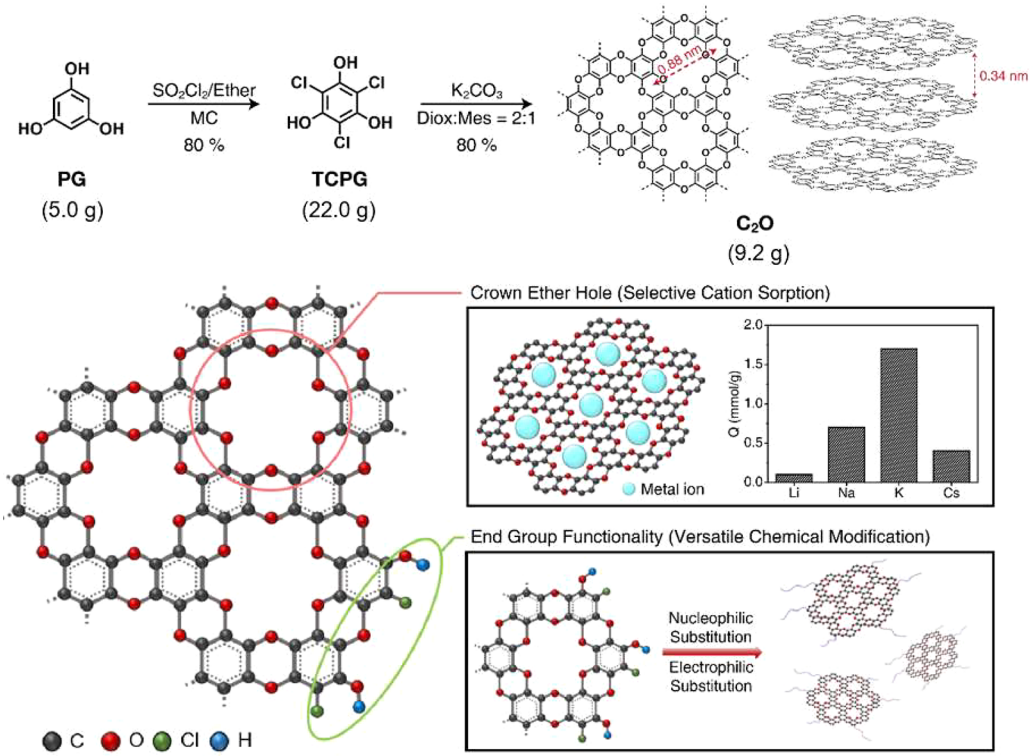

Figure 1. Synthetic strategy for preparing C_2O. Condensation of **TCPG** gives a 2D microporous crystalline framework with pore size of 0.88 nm, denoted C_2O.

sis.[38,39] For example, 18-crown-6 structure is an excellent activated agent for KI in CO_2 fixation with epoxides.[40,41] However, they have limited binding strength and selectivity due to the flexibility of the macrocyclic polyether rings.[42,43] Early studies have established that rigidifying the crown ether structure through chemical modification enhances the binding affinity. For example, Guo et al. found that the crown ether incorporated in graphene generates larger binding energy (~1.4 eV) than those obtained with free crown ether molecules.[44]

Here, we prepare the novel 2D framework having both electrophilic and nucleophilic sites with crown ether holes (C_2O) through irreversible nucleophilic aromatic substitution (S_NAr) of trichlorophloroglucinol (TCPG), where TCPG was prepared by chlorination of phloroglucinol (PG) (Figure 1). The synthesis and the purification of the building unit is facile compared to other reported COFs,[45−47] indicating that the preparation of this 2D material is easily available. C_2O possesses inherent crown ether pores in its rigid skeletal structure, resulting in substantial increases in conversion for cycloaddtion of epoxides with CO_2 by activation of potassium iodide (KI) and improving the nucleophilicity of iodine anions.[48−51] Additionally, C_2O has both electrophilic and nucleophilic sites at the edge of its framework, enabling the precise customization of physicochemical properties through a diverse range of chemical modifications. This offers the advantage of easily introducing desired functional groups and other beneficial properties depending on the applications. Furthermore, C_2O can be produced on a large scale due to the stable stoichiometric balance of TCPG itself and exhibits fine chemical stability under harsh chemical environments by strong covalent bonds formed by self-condensation of TCPG. With its unique combination of scalable, durable, and customizable characteristics, this newly developed covalent framework exhibits immense potential for the design and preparation of outstanding materials with versatile functionalities, making them highly desirable for a wide range of applications.

2. RESULTS AND DISCUSSION

2.1. Preparation of C_2O. The C_2O was simply synthesized by the self-condensation reaction of TCPG with potassium carbonate as a base catalyst, yielding crystalline black precipitates (Figure 1). It is remarkable that the C_2O could be easily prepared on a gram-scale, considering the typical synthesis of COFs by the solvothermal process is limited to only a few hundred milligrams.[52,53] TCPG is a polyfunctional monomer containing stoichiometric amounts of chloride and hydroxyl groups. It is well-known that polymers with high molecular weight could be easily achieved from the polymerization of such monomer type.[54,55] It implies that controlling the polymerization process is likely to further scale up the synthesis of C_2O to the industrial scale. The empirical formula of this product is C_2O for the repeating unit in the basal plane. Elemental analyses were in good agreement with the chemical formula of the molecules (Table S1, Supporting Information). Notably, the material consists of only carbon (C) and oxygen (O) in its skeletal structure; hence, we named the product C_2O. The reaction conversion calculated from the content of residue chloride (0.9% from XPS) is 98.2%. The peak at 200 eV is attributed to the chlorine atoms in the edge of C_2O. Additionally, C_2O could also be prepared through the self-condensation reaction of tribromophloroglucinol (TBPG) as well (see the Supporting Information). However, in this study, C_2O synthesized using TCPG was used for further analysis.

https://doi.org/10.1021/jacs.3c11182
J. Am. Chem. Soc. XXXX, XXX, XXX−XXX

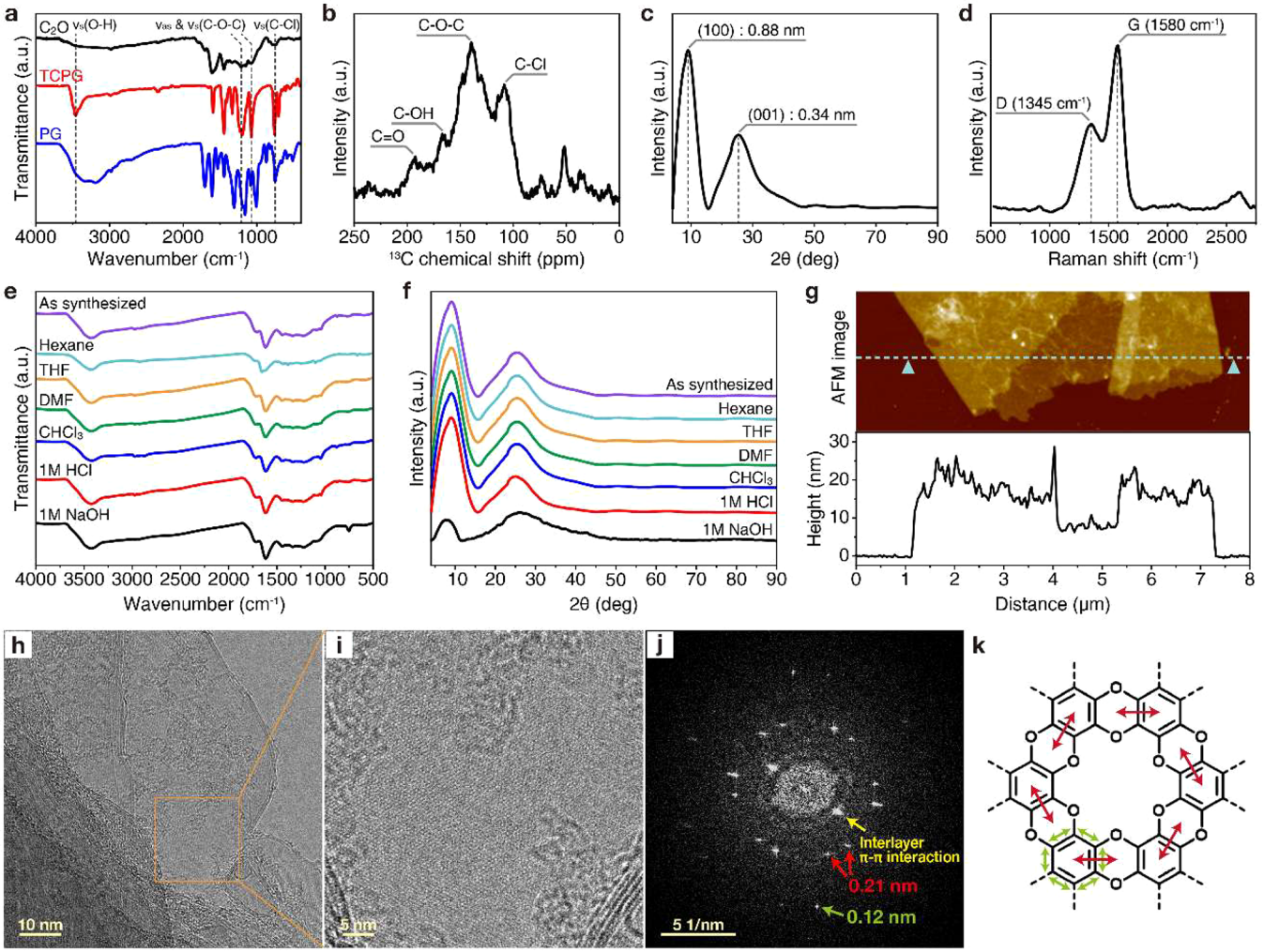

Figure 2. Chracterization of C_2O. (a) FT-IR spectra of **PG** (blue), **TCPG** (red) and C_2O (black). (b) Solid-state ^{13}C CP-MAS NMR spectrum of C_2O. (c) PXRD profile of C_2O. (d) Raman spectrum of C_2O. (e) FT-IR spectra and (f) PXRD patterns of C_2O after treatments under different chemical environments for 1 week. (g) AFM images of C_2O nanosheets with 5−6 nm thickness consisting of ∼18 monolayers. (h) A HR-TEM image of C_2O. (i) A magnified image of the HR-TEM image of the C_2O and (j) its corresponding FFT image. (k) A schematic representation of the C_2O.

By rigidifying crown ethers in a 2D structure, we expect to increase the binding affinity and selective molecule sorption of crown ethers. According to Chisholm et al., the dioxin structure in oxidized graphene is highly stable, which implies that C_2O is a chemically stable material.[44−46] Usually, most COFs have intrinsically limited chemical stability due to their dynamic chemistry that renders these materials chemically vulnerable.[56−58] Unlike these COFs, C_2O is connected by an irreversible dioxin linkage from the self-condensation of TCPG, indicating that much improved chemical stability can be expected. In addition, functional groups such as hydroxyl group and halogen group at the edge of the C_2O allow postmodification with various chemical moieties producing C_2O having different polarities. Furthermore, an ordered inclusion of crown ether holes is expected to coordinate with metal ions[59,60] (K^+, Cu^{2+}, Zn^{2+}, Ce^{3+}, etc.), which would be beneficial for various applications such as catalysis, separation, antibacterial/virus agent, and electrode. In this study, we utilized C_2O as a catalyst for the epoxide cycloaddition reaction with carbon dioxide.

2.2. Characterization of C_2O. Fourier-transform infrared (FT-IR) spectrum of C_2O displays adsorption peaks at 1,240 cm^{-1} and 1,030 cm^{-1}, corresponding to asymmetric and symmetric vibration modes of the ether bonds, respectively (Figure 2a). The significant decrease of the peak intensity in C_2O was observed at 3,458 cm^{-1} (O−H stretching) and 760 cm^{-1} (C−Cl stretching) compared to PG and TCPG, indicating the high conversion of the self-condensation reaction (Figure 2a). The peak intensity of C=O stretching at 1712 cm^{-1} of C_2O was found to be slightly larger than that of TCPG due to the tautomerism of phloroglucinol (PG) derivatives. TCPG shown in Figure 1 is enol-form, while 2,4,6-trichlorocyclohexane-1,3,5-trione can be formed through the tautomerization of TCPG.[61,62] We postulate that the tautomerization of TCPG plays an important role in the formation of C_2O in high conversion. The chloride at the α-position of the carbonyl group formed by the tautomerization is much more reactive than the aryl chloride in TCPG, which facilitates S_NAr reaction (Figure S1, Supporting Information).[63] To further confirm the chemical structure of C_2O, solid-state ^{13}C cross-polarization magic-angle spinning (CP-MAS) NMR spectroscopy was conducted (Figure 2b). The C−O and C−Cl carbon peaks were observed at 146 and 102 ppm, respectively. Additionally, C−OH and C=O carbon

https://doi.org/10.1021/jacs.3c11182
J. Am. Chem. Soc. XXXX, XXX, XXX−XXX

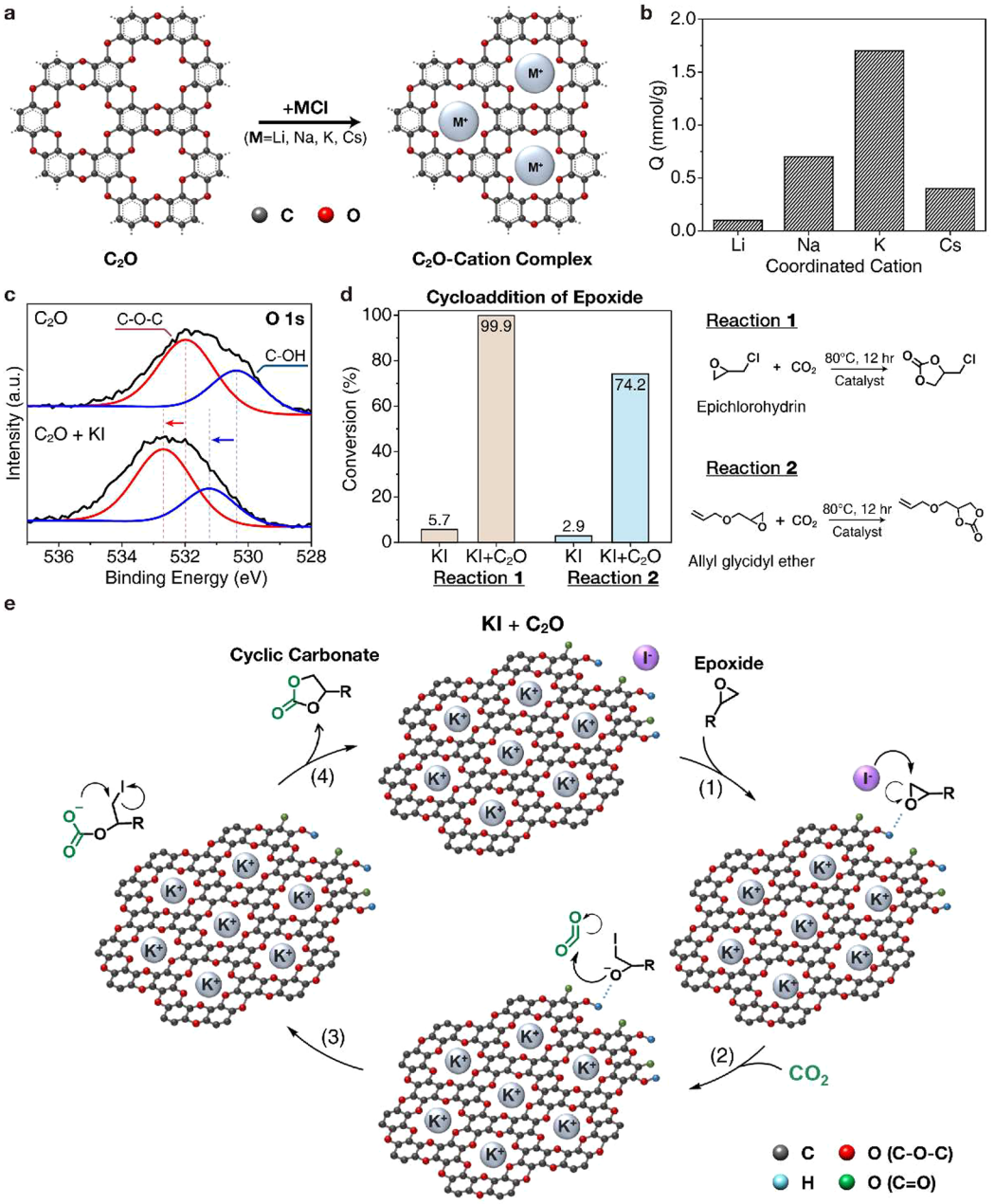

Figure 3. C_2O-catalyzed cycloaddition of epoxides. (a) Schematic illustration of the C_2O-cation complex. (b) Alkali metal ion sorption of C_2O calculated by ICP-MS. (c) O 1s XPS spectra of C_2O and C_2O + KI. (d) Catalytic performance of C_2O with epichlorohydrin and allyl glycidyl ether. (e) The proposed mechanism of the cycloaddition reaction catalyzed by C_2O with KI.

peaks were also observed at 154 and 192 ppm, respectively, with smaller intensity. The peaks below 100 ppm in ^{13}C CPMAS NMR could be attributed to entrapped solvent (or impurities) and satellite peaks.

The powder X-ray diffraction (PXRD) patterns of C_2O show two distinct peaks at 10° and 26°, corresponding to in-plane reflection (100) of 0.88 nm and interlayer distance between stacked sheets of 0.34 nm, respectively (Figure 2c). The experimental PXRD pattern was consistent with the simulated AB stacking mode for 2 layers of C_2O (Figure S2, Supporting Information). The lattice model afforded optimized unit cell with parameters of $a = b = 8.25$ Å, $c = 7.02$ Å, $\alpha = \beta = 90°$, and $\gamma = 60°$. It is noteworthy that C_2O has a crystalline structure even though it was prepared from the irreversible S_NAr reaction. The formation of such a regular 2D structure could be attributable to the rigidity of the building units and strong directionality of the dioxin linkage. The in-plane reflection peak also indicates that C_2O contains crown ether structures rigidified by the backbone frames, which can enhance the binding affinity and selective molecule sorption of crown ethers.[64] The interlayer distance of C_2O is close to that of graphite ($d \approx 0.335$ nm), suggesting that C_2O has a 2D structure close to that of graphene derivatives.[65,66] We also found that potassium ions (K^+) could enhance the crystallinity of C_2O during the self-condensation reaction. Since 18-crown-6, a cyclic crown ether consisting of six ethylene oxide units, is well-known to recognize K^+, it can be assumed that there is a specific interaction of the building unit (TCPG) with potassium ion during the self-condensation reaction. As a result, the peak intensity of the (100) reflection prepared using

https://doi.org/10.1021/jacs.3c11182
J. Am. Chem. Soc. XXXX, XXX, XXX−XXX

K_2CO_3 as base catalyst is larger than that of **C_2O** prepared using triethylamine, indicating that the K^+ acts as a cation template (Figure S3, Supporting Information).[67]

The porous structure of **C_2O** could also be estimated by N_2 adsorption analysis at 77 K (Figure S4, Supporting Information). COFs having large pores prepared from solvothermal process normally show large N_2 uptake, while covalent triazine frameworks (CTF) having smaller pores like **C_2O** show small or no detectable N_2 adsorption, if any. Since CTF and **C_2O** both have a dense structure, N_2 can not be easily adsorbed into the network.[68] Nevertheless, a slight CO_2 uptake of 0.6 mmol·g^{-1} was observed, indicating that hydroxyl groups at the edge of the plane could increase the CO_2 uptake due to hydrophilic interaction. The Raman spectrum of **C_2O** in Figure 2d indicates its graphitic nature by showing two distinct peaks at 1345 cm^{-1} (D band) and 1580 cm^{-1} (G band). The intensity ratio between the D band and G band (I_D/I_G) reflects the disorder of the carbon materials.[69,70] The I_D/I_G value for **C_2O** is 0.64, indicating that **C_2O** has a degree of graphitization higher than that of graphene oxide ($I_D/I_G \approx 0.88$).[71]

The chemical stability of **C_2O** was investigated by treating with various chemical environments such as boiling water, 1 M HCl, 1 M NaOH, chloroform, hexane, and dimethylformamide (DMF) for 7 days. The FT-IR spectra and PXRD patterns of **C_2O** before and after treatment indicated that **C_2O** retains its original structure and crystallinity, demonstrating its fine chemical stability (Figure 2e,f). The thermal stability of **C_2O** was also evaluated using thermogravimetric analysis (TGA) under an N_2 atmosphere, which showed high decomposition temperature and large char yield in comparison to TCPG, indicating the formation of a network structure[72] (Figure S5, Supporting Information). The fine chemical and thermal stabilities of **C_2O** stem from the strong covalent bonding within its structure, achieved through irreversible S_NAr reactions that facilitate the formation of a robust network.

C_2O obtained from the self-condensation reaction and purification process could be easily dispersed by sonication in *N,N*-dimethyl-formamide (DMF) with good dispersity. Atomic force microscopy (AFM) showed that the thickness of the 2D nanosheets was 6 nm, consisting of ∼18 monolayers (Figure 2g). The HR-TEM and corresponding fast Fourier transform (FFT) image of **C_2O** (Figure 2h,j) demonstrate a distinct layered structure with an interlayer distance of 0.34 nm, matching well with the XRD results shown in Figure 2c. In addition, those images represent hexagonal lattices of **C_2O** (Figure 2h−k).

2.3. Catalytic Performance and Postmodification of C_2O. The conversion of CO_2 into value-added products has become an active research field in response to increasing greenhouse gas emissions.[68] It has recently been found that crown ethers are effective phase-transfer agents of potiassium iodide (KI) for the fixation of CO_2 with epoxides, which is alternatively referred to as cycloaddition reaction of CO_2 with epoxides.[40,41] Moreover, hydrogen bond donors such as hydroxyl and amine functional groups were found to facilitate the cycloaddition reaction of CO_2 by activating the epoxides.[70] Given the high density of crown ethers and sufficient hydrogen bond donors, **C_2O** could serve as an attractive cocatalyst for CO_2 fixation (Figure 3a). First, we measured the alkali metal ion sorption properties of **C_2O** using inductively coupled plasma-mass spectrometry (ICP-MS). As shown in Figure 3b, **C_2O** shows the highest ion sorption capacity for the K^+ ion as expected from the pore structure that is the same as 18-crown-6. The K^+ ion adsorption capability was further confirmed by XPS studies. The O 1s XPS spectra of **C_2O** shows two distinct signals at 530.4 and 532.0 eV, which are attributed to the oxygen atoms of crown ether holes and the hydroxyl groups at the edge of the plane, respectively (Figure 3c). Compared to bare **C_2O**, the O 1s spectra of **C_2O** with KI exhibited a shift from 532.0 to 532.7 eV and 530.4 to 531.2 eV due to the interaction between crown ether holes in **C_2O** and K^+, which increased the binding energy of O 1s. (Figure 3c). It has been demonstrated that the coordination of crown ether groups with K^+ can significantly improve the nucleophilicity of I^-.[73,74] Thus, **C_2O** could be a suitable cocatalyst for the cycloaddition of epoxides.

To investigate the catalytic performance of **C_2O**, the cycloadditions of CO_2 with two epoxides (epichlorohydrin and allyl glycidyl ether) were performed (Figure 3d, Table 1).

Table 1. Catalytic Performance of C_2O and Modified-C_2O

Entry	Substrate	Catalyst	Temp. (°C)	Time (h)	Conversion (%)
1	Epichlorohydrin	KI	80	12	5.7
2	Epichlorohydrin	KI + **C_2O** (24 mg)	80	12	**99.9**
3	Allyl glycidyl ether	KI	80	12	2.9
4	Allyl glycidyl ether	KI + **C_2O** (18 mg)	80	12	45.7
5	Allyl glycidyl ether	KI + **C_2O** (24 mg)	80	12	74.2
6	Allyl glycidyl ether	KI + **C_2O** (30 mg)	80	12	75.7
7	Allyl glycidyl ether	KI + **C_2O** (24 mg)	80	18	80.1
8	Allyl glycidyl ether	KI + **C_2O-AGE**[a] (24 mg)	80	12	**97.2**
9	Allyl glycidyl ether	KI + **C_2O-DETA**[b] (24 mg)	80	12	34.8
10	Allyl glycidyl ether	KI + **C_2O-EEA**[c] (24 mg)	80	12	**99.9**

[a]**C_2O** modified with allyl glycidyl ether (see Figure 4a). [b]**C_2O** modified with diethylenetriamine (see Figure S5, Supporting Information). [c]**C_2O** modified with ethoxyethylamine (see Figure 4a).

Potassium iodide (KI) is one of the most extensively studied catalysts in cycloaddtion reaction of epoxides, and it is well-known that the inclusion of the K^+ in the crown ether enhances the catalytic performance of KI due to the increase in nucleophilicity of I^- anion. The use of only KI resulted in relatively low conversion values, such as 5.7 and 2.9% for epichlorohydrin and allyl glycidyl ether, respectively, indicating poor catalytic performance of KI itself. However, the presence of **C_2O** with KI results in remarkable increases in conversion of 99.9% (epichlorohydrin, entry 2 of Table 1) and 74.2% (allyl glycidyl ether, entry 5 of Table 1), which can be ascribed to the crown ethers in the **C_2O** structure.[75,76] Also, recycling studies of **C_2O**−KI-based catalytic system were conducted (Figure S6, Supporting Information) using epichlorohydrin as a substrate, and recycling tests proved that the reaction could be conducted for at least 3 consecutive runs without significant loss of activity, indicating the durability of the **C_2O**−KI based catalytic system. The detailed mechanism of the **C_2O**-catalyzed cycloaddition reaction of CO_2 with epoxides is described in Figure 3e. The nucleophilicity of iodide anion (I^-) is enhanced

https://doi.org/10.1021/jacs.3c11182
J. Am. Chem. Soc. XXXX, XXX, XXX−XXX

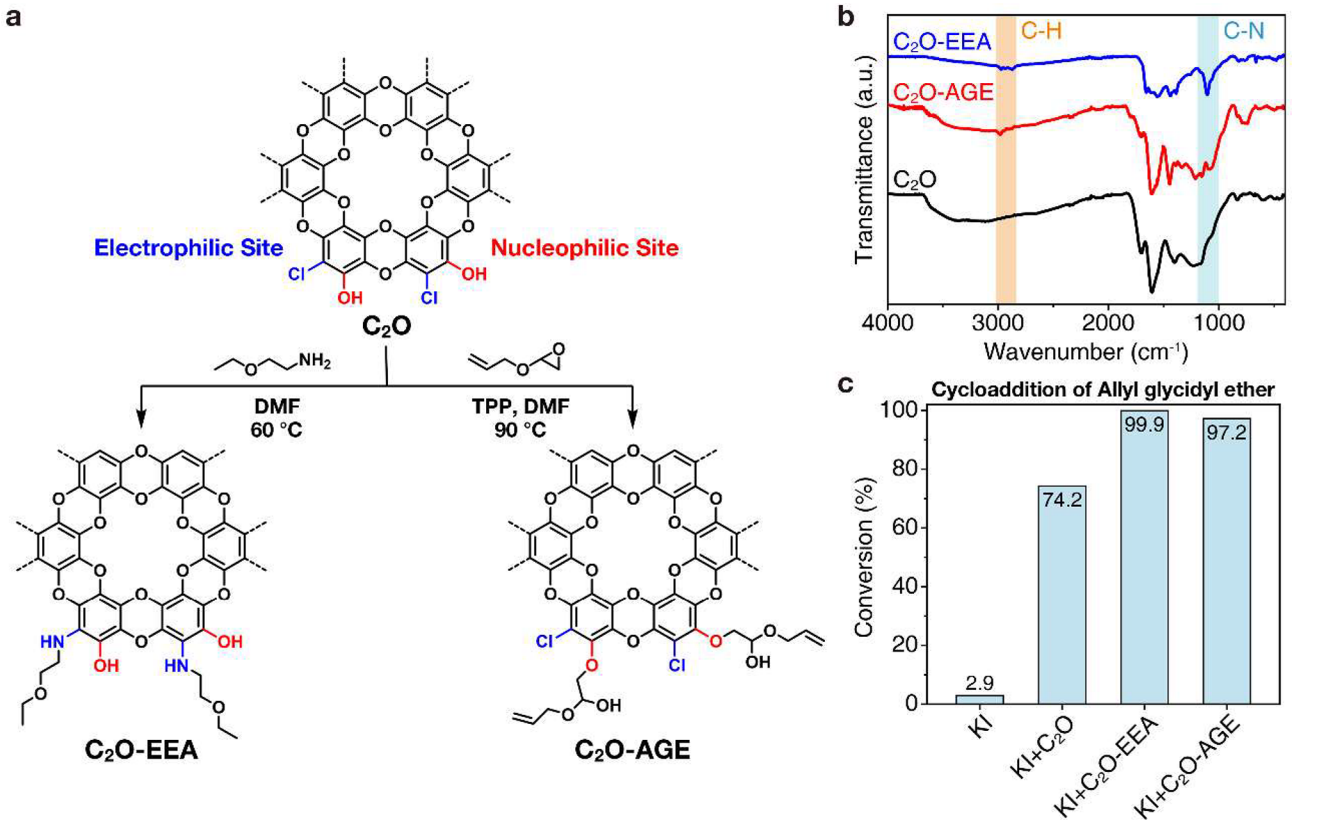

Figure 4. Postmodification of C_2O. (a) The preparation of modified-C_2O using allyl glycidyl ether and 2-ethoxyethylamine (C_2O-**AGE** and C_2O-**EEA**, repectively). (b) The FT-IR spetra of C_2O, C_2O-**AGE**, and C_2O-**EEA**. (c) Catalytic performance of C_2O, C_2O-**AGE**, and C_2O-**EEA**.

by the interaction of C_2O with KI. Additionally, the cycloaddition reaction is facilitated by the hydroxyl groups at the edge of the C_2O, which can activate the epoxides by making them more susceptible to attack by the iodine anion[77] (Figure 3e, (**1**)). The activated epoxide undergoes nucleophilic attack by the iodide anion, leading to the ring opening of the epoxide (Figure 3e, (**2**)). In the next step, the nucleophilic oxygen atom of the epoxide donates a pair of electrons to the electrophilic carbon atom of CO_2, resulting in the formation of a carbon−oxygen bond between the epoxide and CO_2 (Figure 3e, (**3**)). Finally, the intermediate undergoes ring closure to form the cyclic carbonate product, and the catalyst is regenerated to its original form (I^-) to participate in subsequent catalytic cycles (Figure 3e, (**4**)). To gain deeper insight into the catalytic activity of C_2O, the catalytic process is investigated using a density functional theory (DFT) calculation (Figure S7, Supporting Information). In the catalyst-free reaction process, the energy barrier for the RDS (ring opening of epichlorohydrin) is 63.96 kcal/mol, which is consistent with the reported literature[78,79] (Figure S7a, Supporting Information). Similar to the catalyst-free process, the CO_2-epichlorohydrin cycloaddition reaction catalyzed by C_2O was carried out, and the energy profile diagram is shown in Figure S7b, Supporting Information. The ring-opening step is considered the RDS in the CO_2 cycloaddition reaction with an energy barrier of 28.01 kcal/mol, which is significantly lower than that of the reaction without the catalyst (63.96 kcal/mol). The use of C_2O is crucial to promote the desired reaction pathways and offer a sustainable route for the conversion of CO_2 to valuable cyclic carbonates with various applications.

The relatively low conversion with allyl glycidyl ether was attributed to limited compatibility between C_2O and allyl glycidyl ether, which suppresses activation process of the epoxide with C_2O.[80] The conversion of allyl glycidyl ether could be somewhat improved by increasing the reaction time to 18 h (80.1%, entry 7 of Table 1) or by increasing the amount of C_2O to 30 mg (75.7%, entry 6 of Table 1). Nevertheless, the obtained results did not exhibit a dramatic increase, suggesting that further chemical modification of C_2O is necessary to achieve the desired advancement.

To improve the compatibility between C_2O and allyl glycidyl ether, we modified the edge structure of C_2O, utilizing the electrophilic (−Cl) and nucleophilic (−OH) sites located at the edge of the framework (Figure 4a). By incorporating allyl glycidyl ether (AGE) as an electrophile or ethoxyethylamine (EEA) as a nucleophile into C_2O, C_2O-**AGE** and C_2O-**EEA** were successfully synthesized without deformation of their 2D crystalline structure, which was confirmed by FT-IR (Figure 4b) and PXRD results (Figure S8, Supporting Information). It is noteworthy that C_2O can be easily modified with high conversion both by a nucleophile and an electrophile such as EEA and AGE, respectively. This customizable property of C_2O makes it readily amenable to modification with a variety of substrates. The conversion of allyl glycidyl ether was found to be 97.2% and 99.9% (entries 8 and 10) at the same reaction condition when C_2O-**AGE** and C_2O-**EEA** were used for the cycloaddition reaction, respectively (Figure 4c). The increase of the conversion with use of C_2O-**AGE** and C_2O-**EEA** could be attributed to the improved compatibility of the C_2O derivatives in the reaction medium.[81,82] For example, when C_2O-**DETA** (C_2O modified with diethylenetriamine, see

https://doi.org/10.1021/jacs.3c11182
J. Am. Chem. Soc. XXXX, XXX, XXX−XXX

Figure S9, Supporting Information) was used with KI as the catalyst for the cycloaddition reaction of allyl glycidyl ether, the conversion was only 34.8%. Since diethylenetriamine (DETA) has multiple nucleophilic sites, it could cross-link **C_2O** during the modification, leading to poor dispersion of **C_2O-DETA** in the reaction medium. Although quantitative analysis of the miscibility of **C_2O** was not feasible in this study, qualitative analysis was conducted. As shown in Figure S10, it was observed that **C_2O-DETA** showed poor dispersion in the reaction medium, while **C_2O-AGE** and **C_2O-EEA** exhibited much better dispersion in the reaction medium. Between **C_2O-AGE** and **C_2O-EEA**, **C_2O-EEA** demonstrated superior catalytic performance due to the presence of the remaining hydroxyl groups that facilitate the CO_2 fixation reaction.

3. CONCLUSION

In summary, we have successfully synthesized a novel covalent framework, **C_2O**, with crown ether holes in its skeletal structure through irreversible nucleophilic aromatic substitution reaction (S_NAr) of TCPG in a gram-scale. The resulting framework showed a desirable degree of crystallinity with layered 2D structure (d = 0.34 nm) and excellent chemical stability against various chemical environments including acid, base, and different organic solvents. The crown ether holes in the **C_2O** structure were found to strongly coordinate with K^+, thereby increasing the nucleophilicity of I^- and enhancing its catalytic activity for the CO_2 fixation with epoxides. The presence of **C_2O** with KI significantly improves the catalytic performance compared with using KI alone. The catalytic conversion is increased from 5.7% to 99.9% and 2.9% to 74.2% for epichlorohydrin and allyl glycidyl ether, respectively. Since the **C_2O** possesses both electrophilic and nucleophilic sites at the edge of the framework, **C_2O** can be easily modified by incorporating with electrophiles or nucleophiles. For example, **C_2O-AGE** and **C_2O-EEA**, obtained through modification with allyl glycidyl ether and ethoxyethylamine as an electrophile and a nucleophile, respectively, show improved conversions (97.2% and 99.9%) for allyl glycidyl ether compared to unmodified **C_2O** (74.2%). With the unique combination of scalable, durable, and customizable properties of **C_2O**, this newly developed covalent framework holds tremendous potential for the design and preparation of outstanding materials with versatile functionalities, rendering them highly desirable for a wide range of applications, including batteries, fuel cells, purification, antibacterial/antiviral composite materials, etc.

4. EXPERIMENTAL SECTION

4.1. Materials. Phloroglucinol (PG) (≥99%), potassium carbonate (≥99%, Anhydrous), sulfuryl chloride (97%), triethylamine (≥99%), epichlorohydrin (≥99%), allyl glycidyl ether (≥99.0%), N-bromosuccinimide (NBS) (99.0%), diethylenetriamine (99%), 2-ethoxyethylamine (98%), and sodium hydrogen carbonate (≥99.7%) were purchased from Sigma-Aldrich Co., Ltd. (USA). N,N-Dimethylformamide (DMF), diethyl ether, and bromine were purchased from Junsei Co., Ltd. Methylene chloride (MC) was dried with anhydrous calcium chloride, followed by distillation. DMF was used after drying using a molecular sieve (3 Å). All the other reagents were used as received.

4.2. Synthesis of 1,3,5-Trichlorophloroglucinol (TCPG). Typically, 5.0 g (40 mmol) of phloroglucinol (PG) was added into a 250 mL predried round-bottom flask and 10.0 mL of MC was added to prepare PG suspension. 16.2 g (120 mmol) of sulfuryl chloride in 30.0 mL of MC was mixed with the PG suspension. 8.9 g (120 mmol) of diethyl ether was transferred into a dropping funnel and was added dropwise into the mixture under the temperature of 0 °C for 2 h with stirring. After a 2 h reaction, a yellowish solution was obtained without any precipitates. The reaction mixture was dried under vacuum conditions, and then a pinkish powder was obtained. The crude product was dissolved in acetone and then precipitated in deionized water (DIW) 3 times. The product was collected by suction filtration and dried overnight to give an off-white powder (22.0 g, 96 mmol, 80%). mp 154 °C; ^{1}H NMR (300 MHz, DMSO-d_6, δ): δ = 9.912 (OH); ^{13}C NMR (300 MHz, DMSO-d_6, δ): δ = 93.35, 151.30.

4.3. Synthesis of C_2O. A 100 mL RB flask was charged with 5.4 g (40 mmol) of anhydrous K_2CO_3 and 3.0 g (13.1 mmol) of TCPG in a solution of 20.0 mL of dioxane/10.0 mL mesitylene. The flask was flash-frozen at 77 K (LN_2 bath) and evacuated to an internal pressure of 0.15 mmHg. The reaction mixture was heated at 120 °C for 3 days, and the crude product was precipitated in diethyl ether, dilute HCl solution, DIW, and methanol in turn, and the obtained black precipitate was isolated by suction filtration. The dark product was obtained (1.25 g, 80%) and then dried under vacuum conditions at 60 °C overnight.

4.4. Preparation of C_2O-AGE. A 100 mL RB flask was charged with 0.1 g of **C_2O** and 3.0 g of allyl glycidyl ether in a solution of 20.0 mL of DMF. 10 mg of triphenylphosphine was added to the flask, and the reaction mixture was purged with N_2 gas for 10 min. Then, the reaction mixture was heated at 90 °C for 20 h. The crude product was washed with methanol 3 times and isolated by suction filtration. The dark product was obtained and then dried under vacuum conditions at 60 °C overnight.

4.5. Preparation of C_2O-EEA. A 100 mL RB flask was charged with 0.1 g of **C_2O** and 3.0 g of 2-ethoxyethylamine in a solution of 20.0 mL of DMF. The reaction mixture was purged with N_2 gas for 10 min and heated at 90 °C for 20 h. The crude product was washed with methanol 3 times and isolated by suction filtration. The dark product was obtained and then dried under vacuum conditions at 60 °C overnight.

4.6. Catalytic Tests. 10 mmol of epoxides (epichlorohydrin and allyl glycidyl ether) and 0.1 mmol of KI with 24.0 mg/30.0 mg of **C_2O** or without **C_2O** were added into a Schlenk flask. Before the reaction, the reaction system was purged with aqueous CO_2 for 5 min. CO_2 gas was introduced into the flask through a ballon (1 atm), and then, the mixture was reacted at 80 °C for 12 or 18 h with continuous stirring. After the reaction, the product was cooled to room temperature, and the collected sample was centrifuged, filtered, and analyzed by ^{1}H NMR to measure the yields of cyclic carbonates.

4.7. Characterization. The chemical structures were confirmed by ^{1}H NMR and ^{13}C NMR spectroscopy (ZEOL LNM-LA 300, 300 MHz) using DMSO-d_6 (Cambridge Isotope Laboratories) as the NMR solvent and tetramethylsilane (TMS) as the internal standard at room temperature. Fourier transform-infrared (FT-IR) spectra were recorded on a Nicolet 6700 spectrophotometer (Thermo Scientific, USA). Gas chromatography−mass spectrometry (GC-MS) was performed using a magnetic sector instrument by chemical ionization (CI) or by fast atom bombardment (FAB) using the indicated matrix. The elemental contents of carbon, hydrogen, nitrogen, and oxygen were evaluated using Flash2000 (Thermo Fisher Scientific, Germany), an element analyzer (EA). The X-ray photoelectron spectroscopy (XPS) was analyzed with a Sigma probe (Thermo Fisher Scientific, UK) using an Al Kα X-ray source (1486.6 eV). X-ray diffraction (XRD) patterns were taken on a High Power X-ray Diffractometer D/MAZX 2500 V/PC (Cu Kα radiation, 35 kV, 20 mA, 1.5418 Å), Rigaku. Scanning electron microscopy images were taken on a field emission scanning electron microscope (FE-SEM) JSM-7800F Prime (JEOL Ltd., Japan). High-resolution transmission electron microscopy (HR-TEM) images were acquired by using JEM-ARM200F (JEOL Ltd., Japan) under an operating voltage of 80 kV installed at National Center for Inter-University Research Facility (NCIRF) at Seoul National University. The samples for TEM were prepared by drop casting DIW/Acetone dispersion on a Quantifoil holey carbon TEM grid and dried in an oven at 80 °C. The thermal stabilities of the materials were analyzed through thermal gravimetric analysis (TGA) using a TA Instruments TGA Q-500 under a nitrogen (N_2)

https://doi.org/10.1021/jacs.3c11182
J. Am. Chem. Soc. XXXX, XXX, XXX−XXX

atmosphere. The samples were heated to 120 °C at a heating rate of 10 °C/min and maintained at 120 °C for 5 min to remove the remaining moisture and any solvent and then heated to 700 °C at a heating rate of 10 °C/min. The cation sorption experiment was analyzed by inductively coupled plasma optical emission spectroscopy using a 5800 ICP-OES instrument (Agilent).

■ ASSOCIATED CONTENT

Supporting Information

The Supporting Information is available free of charge at https://pubs.acs.org/doi/10.1021/jacs.3c11182.

General methods, synthetic procedures, and characterizations (PDF)

■ AUTHOR INFORMATION

Corresponding Authors

Jungwon Park − *School of Chemical and Biological Engineering, and Institute of Chemical Processes and Institute of Engineering Research, College of Engineering, Seoul National University, Seoul 08826, Republic of Korea; Center for Nanoparticle Research, Institute for Basic Science (IBS), Seoul 08826, Republic of Korea; Advanced Institutes of Convergence Technology, Seoul National University, Gyeonggi-do 16229, Republic of Korea;* orcid.org/0000-0003-2927-4331; Email: jungwonpark@snu.ac.kr

Jong-Chan Lee − *School of Chemical and Biological Engineering, and Institute of Chemical Processes, Seoul National University, Seoul 08826, Republic of Korea;* orcid.org/0000-0002-5587-1183; Email: jongchan@snu.ac.kr

Authors

Jinseok Kim − *School of Chemical and Biological Engineering, and Institute of Chemical Processes, Seoul National University, Seoul 08826, Republic of Korea*

Sungin Kim − *School of Chemical and Biological Engineering, and Institute of Chemical Processes, Seoul National University, Seoul 08826, Republic of Korea; Center for Nanoparticle Research, Institute for Basic Science (IBS), Seoul 08826, Republic of Korea;* orcid.org/0000-0001-9107-0781

Jinwook Park − *School of Chemical and Biological Engineering, and Institute of Chemical Processes, Seoul National University, Seoul 08826, Republic of Korea*

Sungsu Kang − *School of Chemical and Biological Engineering, and Institute of Chemical Processes, Seoul National University, Seoul 08826, Republic of Korea; Center for Nanoparticle Research, Institute for Basic Science (IBS), Seoul 08826, Republic of Korea*

Dong Joo Seo − *School of Chemical and Biological Engineering, and Institute of Chemical Processes, Seoul National University, Seoul 08826, Republic of Korea*

Namjun Park − *School of Chemical and Biological Engineering, and Institute of Chemical Processes, Seoul National University, Seoul 08826, Republic of Korea*

Siyoung Lee − *School of Chemical and Biological Engineering, and Institute of Chemical Processes, Seoul National University, Seoul 08826, Republic of Korea;* orcid.org/0009-0008-6452-1274

Jae Jun Kim − *School of Chemical and Biological Engineering, and Institute of Chemical Processes, Seoul National University, Seoul 08826, Republic of Korea*

Won Bo Lee − *School of Chemical and Biological Engineering, and Institute of Chemical Processes, Seoul National University, Seoul 08826, Republic of Korea;* orcid.org/0000-0001-7801-083X

Complete contact information is available at: https://pubs.acs.org/10.1021/jacs.3c11182

Notes

The authors declare no competing financial interest.

■ ACKNOWLEDGMENTS

This research was supported by the National Research Foundation of Korea (NRF-2020R1A2C2008114 and NRF-2018R1A5A1024127).

■ REFERENCES

(1) Wang, Z.; Zhang, S.; Chen, Y.; Zhang, Z.; Ma, S. Covalent organic frameworks for separation applications. *Chem. Soc. Rev.* **2020**, *49*, 708−735.

(2) Guan, X.; Ma, Y.; Li, H.; Yusran, Y.; Xue, M.; Fang, Q.; Yan, Y.; Valtchev, V.; Qiu, S. Fast, Ambient Temperature and Pressure Ionothermal Synthesis of Three-Dimensional Covalent Organic Frameworks. *J. Am. Chem. Soc.* **2018**, *140* (13), 4494−4498.

(3) Dey, K.; Pal, M.; Rout, K. C.; Kunjattu H, S.; Das, H. A.; Mukherjee, R.; Kharul, U. K.; Banerjee, R. Selective Molecular Separation by Interfacially Crystallized Covalent Organic Framework Thin Films. *J. Am. Chem. Soc.* **2017**, *139*, 13083−13091.

(4) Feng, X.; Ding, X.; Jiang, D. Covalent organic frameworks. *Chem. Soc. Rev.* **2012**, *41*, 6010−6022.

(5) Han, S. S.; Furukawa, H.; Yaghi, O. M.; Goddard, W. A. Covalent Organic Frameworks as Exceptional Hydrogen Storage Materials. *J. Am. Chem. Soc.* **2008**, *130* (35), 11580−11581.

(6) Gottschling, K.; Stegbauer, L.; Savasci, G.; Prisco, N. A.; Berkson, Z. J.; Ochsenfeld, C.; Chmelka, B. F.; Lotsch, B. V. Molecular Insights into Carbon Dioxide Sorption in Hydrazone-Based Covalent Organic Frameworks with Tertiary Amine Moieties. *Chem. Mater.* **2019**, *31* (6), 1946−1955.

(7) Kuhn, P.; Antonietti, M.; Thomas, A. Porous, Covalent Triazine-Based Frameworks Prepared by Ionothermal Synthesis. *Angew. Chem., Int. Ed.* **2008**, *47* (18), 3450−3453.

(8) Wang, S.; Wang, Q.; Shao, P.; Han, Y.; Gao, X.; Ma, L.; Yuan, S.; Ma, X.; Zhou, J.; Feng, X.; Wang, B. Exfoliation of Covalent Organic Frameworks into Few-Layer Redox-Active Nanosheets as Cathode Materials for Lithium-Ion Batteries. *J. Am. Chem. Soc.* **2017**, *139* (12), 4258−4261.

(9) Lei, Z.; Yang, Q.; Xu, Y.; Guo, S.; Sun, W.; Liu, H.; Lv, L. P.; Zhang, Y.; Wang, Y. Boosting lithium storage in covalent organic framework via activation of 14-electron redox chemistry. *Nat. Commun.* **2018**, *9* (1), 576.

(10) Liu, J.; Lyu, P.; Zhang, Y.; Nachtigall, P.; Xu, Y. New Layered Triazine Framework/Exfoliated 2D Polymer with Superior Sodium-Storage Properties. *Adv. Mater.* **2018**, *30*, No. 1705401.

(11) Luo, Z.; Liu, L.; Ning, J.; Lei, K.; Lu, Y.; Li, F.; Chen, J. A Microporous Covalent−Organic Framework with Abundant Accessible Carbonyl Groups for Lithium-Ion Batteries. *Angew. Chem., Int. Ed.* **2018**, *57*, 9443−9446.

(12) Montoro, C.; Rodríguez-San-Miguel, D.; Polo, E.; Escudero-Cid, R.; Ruiz-González, M. L.; Navarro, J. A. R.; Ocón, P.; Zamora, F. Ionic Conductivity and Potential Application for Fuel Cell of a Modified Imine-Based Covalent Organic Framework. *J. Am. Chem. Soc.* **2017**, *139* (29), 10079−10086.

(13) Sun, Q.; Aguila, B.; Perman, J.; Nguyen, N.; Ma, S. Flexibility Matters: Cooperative Active Sites in Covalent Organic Framework and Threaded Ionic Polymer. *J. Am. Chem. Soc.* **2016**, *138* (48), 15790−15796.

(14) Xu, H.; Gao, J.; Jiang, D. Stable, crystalline, porous, covalent organic frameworks as a platform for chiral organocatalysts. *Nat. Chem.* **2015**, *7* (11), 905−912.
(15) Ding, S. Y.; Gao, J.; Wang, Q.; Zhang, Y.; Song, W. G.; Su, C. Y.; Wang, W. Construction of Covalent Organic Framework for Catalysis: Pd/COF-LZU1 in Suzuki−Miyaura Coupling Reaction. *J. Am. Chem. Soc.* **2011**, *133* (49), 19816−19822.
(16) Wang, X.; Han, X.; Zhang, J.; Wu, X.; Liu, Y.; Cui, Y. Homochiral 2D Porous Covalent Organic Frameworks for Heterogeneous Asymmetric Catalysis. *J. Am. Chem. Soc.* **2016**, *138* (38), 12332−12335.
(17) Du, Y. R.; Ding, G. R.; Wang, Y. F.; Xu, B. H.; Zhang, S. J. Construction of a PPIL@COF core−shell composite with enhanced catalytic activity for CO_2 conversion. *Green Chem.* **2021**, *23*, 2411.
(18) Côté, A. P.; Benin, A. I.; Ockwig, N. W.; O'Keeffe, M.; Matzger, A. J.; Yaghi, O. M. Porous, Crystalline, Covalent Organic Frameworks. *Science* **2005**, *310* (5751), 1166−1170.
(19) Lohse, M. S.; Bein, T. Covalent Organic Frameworks: Structures, Synthesis, and Applications. *Adv. Funct. Mater.* **2018**, *28*, No. 1705553.
(20) Wang, H.; Zeng, Z.; Xu, P.; Li, L.; Zeng, G.; Xiao, R.; Tang, Z.; Huang, D.; Tang, L.; Lai, C.; Jiang, D.; Liu, Y.; Yi, H.; Qin, L.; Ye, S.; Ren, X.; Tang, W. Recent progress in covalent organic framework thin films: fabrications, applications and perspectives. *Chem. Soc. Rev.* **2019**, *48*, 488−516.
(21) Hamzehpoor, E.; Jonderian, A.; McCalla, E.; Perepichka, D. F. Synthesis of Boroxine and Dioxaborole Covalent Organic Frameworks via Transesterification and Metathesis of Pinacol Boronates. *J. Am. Chem. Soc.* **2021**, *143* (33), 13274−13280.
(22) Chen, X.; Zhang, H.; Ci, C.; Sun, W.; Wang, Y. Few-Layered Boronic Ester Based Covalent Organic Frameworks/Carbon Nanotube Composites for High-Performance K-Organic Batteries. *ACS Nano* **2019**, *13* (3), 3600−3607.
(23) Uribe-Romo, F. J.; Doonan, C. J.; Furukawa, H.; Oisaki, K.; Yaghi, O. M. Crystalline Covalent Organic Frameworks with Hydrazone Linkages. *J. Am. Chem. Soc.* **2011**, *133* (30), 11478−11481.
(24) Uribe-Romo, F. J.; Hunt, J. R.; Furukawa, H.; Klöck, C.; O'Keeffe, M.; Yaghi, O. M. A Crystalline Imine-Linked 3-D Porous Covalent Organic Framework. *J. Am. Chem. Soc.* **2009**, *131* (13), 4570−4571.
(25) Qian, C.; Feng, L.; Teo, W. L.; Liu, J.; Zhou, W.; Wang, D.; Zhao, Y. Imine and imine-derived linkages in two-dimensional covalent organic frameworks. *Nat. Rev. Chem.* **2022**, *6* (12), 881−898.
(26) Fang, Q.; Zhuang, Z.; Gu, S.; Kaspar, R. B.; Zheng, J.; Wang, J.; Qiu, S.; Yan, Y. Designed synthesis of large-pore crystalline polyimide covalent organic frameworks. *Nat. Commun.* **2014**, *5* (1), 4503.
(27) Chandra, S.; Kundu, T.; Dey, K.; Addicoat, M.; Heine, T.; Banerjee, R. Interplaying Intrinsic and Extrinsic Proton Conductivities in Covalent Organic Frameworks. *Chem. Mater.* **2016**, *28*, 1489−1494.
(28) Kandambeth, S.; Venkatesh, V.; Shinde, D. B.; Kumari, S.; Halder, A.; Verma, S.; Banerjee, R. Self-templated chemically stable hollow spherical covalent organic framework. *Nat. Commun.* **2015**, *6* (1), 6786.
(29) Kandambeth, S.; Mallick, A.; Lukose, B.; Mane, M. V.; Heine, T.; Banerjee, R. Construction of Crystalline 2D Covalent Organic Frameworks with Remarkable Chemical (Acid/Base) Stability via a Combined Reversible and Irreversible Route. *J. Am. Chem. Soc.* **2012**, *134* (48), 19524−19527.
(30) Wu, X.; Han, X.; Liu, Y.; Liu, Y.; Cui, Y. Control Interlayer Stacking and Chemical Stability of Two-Dimensional Covalent Organic Frameworks via Steric Tuning. *J. Am. Chem. Soc.* **2018**, *140* (47), 16124−16133.
(31) Kan, X.; Wang, J. C.; Kan, J. L.; Shang, J. Y.; Qiao, H.; Dong, Y. B. Gram-Scale Synthesis of Cu(II)@COF via Solid-State Coordination Approach for Catalysis of Alkyne-Dihalomethane-Amine Coupling. *Inorg. Chem.* **2021**, *60* (5), 3393−3400.
(32) Lu, J.; Lin, F.; Wen, Q.; Qi, Q. Y.; Xu, J. Q.; Zhao, X. Large-scale synthesis of azine-linked covalent organic frameworks in water and promoted by water. *New J. Chem.* **2019**, *43*, 6116.
(33) Steed, J. W. First- and second-sphere coordination chemistry of alkali metal crown ether complexes. *Coord. Chem. Rev.* **2001**, *215* (1), 171−221.
(34) Oral, I.; Abetz, V. Improved alkali metal ion capturing utilizing crown ether-based diblock copolymers in a sandwich-type complexation. *Soft Matter* **2022**, *18* (5), 934−937.
(35) Awual, M. R. Ring size dependent crown ether based mesoporous adsorbent for high cesium adsorption from wastewater. *Chemical Engineering Journal* **2016**, *303*, 539−546.
(36) Iannazzo, D.; Espro, C.; Ferlazzo, A.; Celesti, C.; Branca, C.; Neri, G. Electrochemical and Fluorescent Properties of Crown Ether Functionalized Graphene Quantum Dots for Potassium and Sodium Ions Detection. *Nanomaterials* **2021**, *11* (11), 2897.
(37) Kralj, M.; Tušek-Božić, L.; Frkanec, L. Biomedical Potentials of Crown Ethers: Prospective Antitumor Agents. *ChemMedChem.* **2008**, *3* (10), 1478−1492.
(38) Cacciapaglia, R.; Mandolins, L. Catalysis by metal ions in reactions of crown ether substrates. *Chem. Soc. Rev.* **1993**, *22* (4), 221−231.
(39) Yoo, C.; Dodge, H. M.; Miller, A. J. M. Cation-controlled catalysis with crown ether-containing transition metal complexes. *Chem. Commun.* **2019**, *55* (35), 5047−5059.
(40) Desens, W.; Kohrt, C.; Frank, M.; Werner, T. Highly Efficient Polymer-Supported Catalytic System for the Valorization of Carbon Dioxide. *ChemSusChem* **2015**, *8*, 3815−3822.
(41) Hao, Y.; Yan, X.; Chang, T.; Liu, X.; Kang, L.; Zhu, Z.; Panchal, B.; Qin, S. Hydroxyl-anchored covalent organic crown-based polymers for CO_2 fixation into cyclic carbonates under mild conditions. *Sustainable Energy & Fuels* **2021**, *6* (1), 121−127.
(42) Cram, D. J. The Design of Molecular Hosts, Guests, and Their Complexes. *Angew. Chem., Int. Ed.* **1988**, *27*, 1009−1020.
(43) Hay, B. P.; Rustad, J. R.; Hostetler, C. J. Quantitative structure-stability relationship for potassium ion complexation by crown ethers. A molecular mechanics and ab initio study. *J. Am. Chem. Soc.* **1993**, *115*, 11158.
(44) Guo, J.; Lee, J.; Contescu, C. I.; Gallego, N. C.; Pantelides, S. T.; Pennycook, S. J.; Moyer, B. A.; Chisholm, M. F. Crown ethers in graphene. *Nat. Commun.* **2014**, *5*, 5389.
(45) Li, J.; Lan, J.; Cao, R.; Sun, J.; Ding, X.; Liu, X.; Yuan, L.; Shi, W. Water-Mediated Hydrogen Bond Network Drives Highly Crystalline Structure Formation of Crown Ether-Based Covalent Organic Framework for Sr Adsorption. *ACS Appl. Mater. Interfaces* **2023**, *15*, 59544.
(46) Han, D.; Sun, L.; Li, Z.; Qin, W.; Zhai, L.; Sun, Y.; Tang, S.; Fu, Y. Supramolecular channels via crown ether functionalized covalent organic frameworks for boosting polysulfides conversion in Li− S batteries. *Energy Storage Materials* **2024**, *65*, 103143.
(47) Gu, X.; Wang, B.; Pang, Y.; Zhu, H.; Wang, R.; Chen, T.; Li, Y.; Yan, X. Crown ether-based covalent organic frameworks for CO_2 fixation. *New J. Chem.* **2023**, *47*, 2040.
(48) Zhang, B.; Wei, M.; Mao, H.; Pei, X.; Alshmimri, S. A.; Reimer, J. A.; Yaghi, O. M. Crystalline Dioxin-Linked Covalent Organic Frameworks from Irreversible Reactions. *J. Am. Chem. Soc.* **2018**, *140*, 12715−12719.
(49) Guan, X.; Li, H.; Ma, Y.; Xue, M.; Fang, Q.; Yan, Y.; Valtchev, V.; Qiu, S. Chemically stable polyarylether-based covalent organic frameworks. *Nat. Chem.* **2019**, *11* (6), 587−594.
(50) An, S.; Xu, Q.; Ni, Z.; Hu, J.; Peng, C.; Zhai, L.; Guo, Y.; Liu, H. Construction of Covalent Organic Frameworks with Crown Ether Struts. *Angew. Chem., Int. Ed.* **2021**, *60*, 9959−9963.
(51) Shen, J. C.; Jiang, W. L.; Guo, W. D.; Qi, Q. Y.; Ma, D. L.; Lou, X.; Shen, M.; Hu, B.; Yang, H. B.; Zhao, X. A rings-in-pores net: crown ether-based covalent organic frameworks for phase-transfer catalysis. *Chem. Commun.* **2020**, *56*, 595−598.

https://doi.org/10.1021/jacs.3c11182
J. Am. Chem. Soc. XXXX, XXX, XXX−XXX

(52) Lin, G.; Ding, H.; Chen, R.; Peng, Z.; Wang, B.; Wang, C. 3D Porphyrin-Based Covalent Organic Frameworks. *J. Am. Chem. Soc.* **2017**, *139*, 8705−8709.
(53) Zhang, Y.; Duan, J.; Ma, D.; Li, P.; Li, S.; Li, H.; Zhou, J.; Ma, X.; Feng, X.; Wang, B. Three-Dimensional Anionic Cyclodextrin-Based Covalent Organic Frameworks. *Angew. Chem., Int. Ed.* **2017**, *56*, 16313−16317.
(54) Lunt, J. Large-scale production, properties and commercial applications of polylactic acid polymers. *Polym. Degrad. Stab.* **1998**, *59*, 145−152.
(55) Kory, M. J.; Worle, M.; Weber, T.; Payamyar, P.; van de Poll, S. W.; Dshemuchadse, J.; Trapp, N.; Schluter, A. D. Gram-scale synthesis of two-dimensional polymer crystals and their structure analysis by X-ray diffraction. *Nat. Chem.* **2014**, *6*, 779−784.
(56) Qian, C.; Feng, L.; Teo, W. L.; Liu, J.; Zhou, W.; Wang, D.; Zhao, Y. Imine and imine-derived linkages in two-dimensional covalent organic frameworks. *Nature Reviews Chemistry* **2022**, *6*, 881−898.
(57) Sun, Q.; Aguila, B.; Perman, J.; Earl, L. D.; Abney, C. W.; Cheng, Y.; Wei, H.; Nguyen, N.; Wojtas, L.; Ma, S. Postsynthetically Modified Covalent Organic Frameworks for Efficient and Effective Mercury Removal. *J. Am. Chem. Soc.* **2017**, *139*, 2786−2793.
(58) Uribe-Romo, F. J.; Hunt, J. R.; Furukawa, H.; Klock, C.; O'Keeffe, M.; Yaghi, O. M. A Crystalline Imine-Linked 3-D Porous Covalent Organic Framework. *J. Am. Chem. Soc.* **2009**, *131*, 4570−4571.
(59) Mohamed, M. G.; Chang, W. C.; Kuo, S. W. Crown Ether- and Benzoxazine-Linked Porous Organic Polymers Displaying Enhanced Metal Ion and CO2 Capture through Solid-State Chemical Transformation. *Macromolecules* **2022**, *55*, 7879−7892.
(60) Yuan, L.; Zhu, J.; Wu, S.; Chi, C. Enhanced emission by stacking of crown ether side chains in a 2D covalent organic framework. *Chem. Commun.* **2022**, *58*, 1302.
(61) Zali-Boeini, H.; Mansouri, S. G. Tribromo Phloroglucinol as a Novel and Highly Efficient Reagent for the Conversion of Benzothioamides to the Corresponding 1,2,4-Thiadiazoles. *Synth. Commun.* **2015**, *45*, 1681−1687.
(62) Lohrie, M.; Knoche, W. Dissociation and keto-enol tautomerism of phloroglucinol and its anions in aqueous solution. *J. Am. Chem. Soc.* **1993**, *115*, 919−924.
(63) Highet, R. J.; Ekhato, I. V. Keto-enol tautomerism of phloroglucinol and the formation of the tris(sodium bisulfite) addition complex. *J. Org. Chem.* **1988**, *53*, 2843−2844.
(64) Kaewmee, P.; Manyam, J.; Opaprakasit, P.; TrucLe, G. T.; Chanlek, N.; Sreearunothai, P. Effective removal of cesium by pristine graphene oxide: performance, characterizations and mechanisms. *RSC Adv.* **2017**, *7*, 38747.
(65) Jeong, H. K.; Lee, Y. P.; Lahaye, R. J. W. E.; Park, M. H.; An, K. H.; Kim, I. J.; Yang, C. W.; Park, C. Y.; Ruoff, R. S.; Lee, Y. H. Evidence of Graphitic AB Stacking Order of Graphite Oxides. *J. Am. Chem. Soc.* **2008**, *130*, 1362−1366.
(66) Kim, D. S.; Kwon, H.; Nikitin, A. Y.; Ahn, S.; Martin-Moreno, L.; Garcia-Vidal, F. J.; Ryu, S.; Min, H.; Kim, Z. H. Stacking Structures of Few-Layer Graphene Revealed by Phase-Sensitive Infrared Nanoscopy. *ACS Nano* **2015**, *9* (7), 6765−6773.
(67) Terashima, T.; Kawabe, M.; Miyabara, Y.; Yoda, H.; Sawamoto, M. Polymeric pseudo-crown ether for cation recognition via cation template-assisted cyclopolymerization. *Nat. Commun.* **2013**, *4*, 2321.
(68) Katekomol, P.; Roeser, J.; Bojdys, M.; Weber, J.; Thomas, A. Covalent Triazine Frameworks Prepared from 1,3,5-Tricyanobenzene. *Chem. Mater.* **2013**, *25*, 1542−1548.
(69) Scardaci, V.; Compagnini, G. Raman Spectroscopy Investigation of Graphene Oxide Reduction by Laser Scribing. *C* **2021**, *7*, 48.
(70) Malard, L. M.; Pimenta, M. A.; Dresselhaus, G.; Dresselhaus, M. S. Raman spectroscopy in graphene. *Physical Reports* **2009**, *473*, 51−87.
(71) Claramunt, S.; Varea, A.; Lopez-Diaz, D.; Mercedes Velazquez, M.; Cornet, A.; Cirera, A. The Importance of Interbands on the Interpretation of the Raman Spectrum of Graphene Oxide. *J. Phys. Chem. C* **2015**, *119* (18), 10123−10129.
(72) Shin, H.; Kim, D.; Kim, H. J.; Kim, J.; Char, K.; Yavuz, C. T.; Choi, J. W. Fluorinated Covalent Organic Polymers for High Performance Sulfur Cathodes in Lithium−Sulfur Batteries. *Chem. Mater.* **2019**, *31* (19), 7910−7921.
(73) Steinbauer, J.; Werner, T. Poly(ethylene glycol)s as Ligands in Calcium-Catalyzed Cyclic Carbonate Synthesis. *ChemSusChem* **2017**, *10*, 3025−3029.
(74) Steinbauer, J.; Spannenberg, A.; Werner, T. An in situ formed Ca^{2+}−crown ether complex and its use in CO_2-fixation reactions with terminal and internal epoxides. *Green Chem.* **2017**, *19*, 3769−3779.
(75) Kaneko, S.; Shirakawa, S. Potassium Iodide−Tetraethylene Glycol Complex as a Practical Catalyst for CO_2 Fixation Reactions with Epoxides under Mild Conditions. *ACS Sustainable Chem. Eng.* **2017**, *5*, 2836−2840.
(76) Du, Y. R.; Ding, G. R.; Wang, Y. F.; Xu, B. H.; Zhang, S. J. Construction of a PPIL@COF core−shell composite with enhanced catalytic activity for CO2 conversion. *Green Chem.* **2021**, *23*, 2411.
(77) Ding, L. G.; Yao, B. J.; Li, F.; Shi, S. C.; Huang, N.; Yin, H. B.; Guan, Q.; Dong, Y. B. Ionic liquid-decorated COF and its covalent composite aerogel for selective CO_2 adsorption and catalytic conversion. *J. Mater. Chem. A* **2019**, *7*, 4689.
(78) Steinbauer, J.; Spannenberg, A.; Werner, T. An in situ formed Ca^{2+}−crown ether complex and its use in CO_2-fixation reactions with terminal and internal epoxides. *Green Chem.* **2017**, *19*, 3769−3779.
(79) Kurisingal, J.-F.; Li, Y.; Sagynbayeva, Y.; Chitumalla, R.-K.; Vuppala, S.; Rachuri, Y.; Gu, Y.; Jang, J.; Park, D.-W. Porous aluminum-based DUT metal-organic frameworks for the transformation of CO2 into cyclic carbonates: a computationally supported study. *Catal. Today* **2020**, *352*, 227−236.
(80) Yin, M.; Wang, L.; Tang, S. Amino-Functionalized Ionic-Liquid-Grafted Covalent Organic Frameworks for High-Efficiency CO_2 Capture and Conversion. *ACS Appl. Mater. Interfaces* **2022**, *14*, 55674−55685.
(81) Saptal, V.; Shinde, D. B.; Banerjee, R.; Bhanage, B. M. State-of-the-art catechol porphyrin COF catalyst for chemical fixation of carbon dioxide via cyclic carbonates and oxazolidinones. *Catal. Sci. Technol.* **2016**, *6*, 6152.
(82) Zhi, Y.; Shao, P.; Feng, X.; Xia, H.; Zhang, Y.; Shi, Z.; Mu, Y.; Liu, X. Covalent organic frameworks: efficient, metal-free, heterogeneous organocatalysts for chemical fixation of CO_2 under mild conditions. *J. Mater. Chem. A* **2018**, *6*, 374.

https://doi.org/10.1021/jacs.3c11182
J. Am. Chem. Soc. XXXX, XXX, XXX−XXX